

dependence of $\Delta p/L$ on M may be more complicated than Eq. (A1) indicates.

Equation (A9) predicts $\Delta p/L \propto I/p$, just as Rüttenauer observed, but unfortunately the use of the high-pressure form for V_3 in Eq. (A8) [which leads to Eq. (A9)] cannot be justified in the case of helium and neon. The critical value of pR separating the high-pressure and low-pressure forms for V_3 may be written

$$pR \approx 1.06V_e$$

(p in Torr, R in mm, V_e in V) in argon. However, according to Francis, V_e ranges from 5 to 15 V for helium and neon in Rüttenauer's experiments. (Such high electron temperatures have been observed by Labuda and Gordon³⁰ in helium-neon discharges.) Physically, this then means that the radial fields are much greater in helium and neon than in argon at similar values of pR , so that ion radial drift velocities are considerably greater in the lighter gases at a given value of pR . Thus V_3 will still have its "small x " form at some values of pR in argon but its "large x " form at the same values of pR in neon or helium.

Specifically, one finds that the crossover from the high-pressure form of V_3 to the low-pressure form

³⁰E. F. Labuda and E. I. Gordon, J. Appl. Phys. 35, 1647 (1964).

should occur at

$$pR \approx 2.02V_e \text{ in neon}$$

and

$$pR \approx 2.22V_e \text{ in helium}$$

(p in Torr, R in mm, V_e in V). If the high values of electron temperature previously mentioned occurred in Rüttenauer's tubes, then it is clear that the appropriate form for V_3 in Eq. (A7) should be the low-pressure form (the large- x limit). As previously remarked in the case of argon, the large- x limit of V_3 is pressure-independent, so that the $1/p$ dependence found by Rüttenauer cannot be accounted for in this case.

The resolution of this remaining disagreement must await further work. Perhaps the electron temperature in Rüttenauer's range of current and pressures is lower than estimated here, in which case Eq. (A9) would still be applicable and would account for his measurements in helium and neon. Perhaps other pumping processes at work in these gases make V_3 an incomplete description of the pumping mechanism. Or perhaps, because of the small currents used by Rüttenauer, changes in electron temperature and axial field as a function of current obscured a true interpretation of the pressure dependence over the limited range of parameters he used in his work on helium and neon.

Asymptotic Electric Microfield Distributions in Low-Frequency Component Plasmas*

C. F. HOOPER, JR.

Department of Physics and Astronomy, University of Florida, Gainesville, Florida

(Received 21 December 1967)

A recently developed collective-coordinate technique is employed to calculate electric microfield distribution functions $P(\epsilon)$ for low-frequency-component plasmas. Values of ϵ considered range from 10 to 50, and both neutral-point and charged-point cases are treated. Comparison is made with appropriate asymptotic expressions.

I. INTRODUCTION

RECENTLY, a collective-coordinate technique has been used to calculate electric microfield distributions in plasmas; both high-frequency- and low-frequency-component plasmas were considered.^{1,2} The distribution functions graphed and tabulated in these papers were for values of field strength ϵ measured in

units of the normal field strength, from zero to 10. However, for a number of practical applications such as spectral line broadening in plasmas, there is need for values of the microfield distribution function $P(\epsilon)$ for values of ϵ greater than 10.

It is the purpose of this paper to calculate and discuss the low-frequency-component microfield distribution functions for values of ϵ between 10 and 50. Both the neutral- and charged-point cases will be treated. Much of the work presented in this paper is based on the formalism developed in Refs. 1 and 2, hereafter referred to as I and II, respectively.

* This research was supported in part by the National Aeronautics and Space Administration.

¹ C. F. Hooper, Jr., Phys. Rev. 149, 77 (1966).

² C. F. Hooper, Jr., Phys. Rev. 165, 215 (1968).

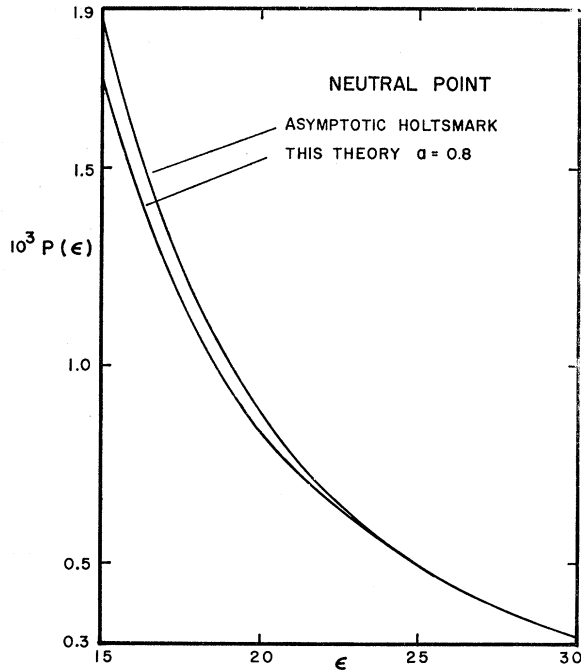


FIG. 1. A comparison of the neutral-point electric microfield distribution function calculated using the theory developed in II, with the asymptotic Holtsmark result; ϵ is in units of ϵ_0 .

II. RESULTS AND DISCUSSION

The results will be divided into two categories: the charged-point case and the neutral-point case. The latter will be considered first.

Electric microfield distribution functions $P(\epsilon)$ at a neutral point in the low-frequency-component plasma were calculated using Eqs. (1), (16), (17), and (18) of II, for several values of a , and for an ϵ range of from 10 to 50. The results were then compared with the asymptotic Holtsmark expression given by³

$$P(\epsilon)_{\text{asymptotic}} = 1.496\epsilon^{-5/2} + 7.639\epsilon^{-4} + 21.60\epsilon^{-11/2} + \dots \quad (1)$$

This comparison indicated that before the point $\epsilon=30$ is reached, all four $P(\epsilon)$ curves join with the asymptotic Holtsmark expression. An example of this is graphically illustrated in Fig. 1. Values of $P(\epsilon)$ calculated with the more exact formalism are tabulated in Table I together with those calculated with Eq. (1). In every case, with at most an error of a few percent, neutral-point $P(\epsilon)$ values for $\epsilon > 30$ can be found, using Eq. (1). In fact, for the $a=0.2$ case, $P(\epsilon)$ values for $\epsilon > 20$ can be found using Eq. (1).

To calculate $P(\epsilon)$ at a charged point (e.g., at an ion) in the low-frequency-component plasma, use is made of Eqs. (1), (13), (15), and (16) in II. Again, ϵ values range between 10 and 50. To calculate an expression

TABLE I. Probability distributions $10^3P(\epsilon)$ at a neutral point, for several values of a , compared with the asymptotic Holtsmark results [see Eq. (1) in text]. The electric-field strength ϵ is expressed in units of ϵ_0 . In each $10^3P(\epsilon)$ column characterized by a given a value, values are listed until they coincide with the corresponding asymptotic result to within a few percent. Therefore, for all $10^3P(\epsilon)$ values not explicitly listed, the asymptotic results should be used.

ϵ	$a=0.2$	$a=0.4$	$a=0.6$	$a=0.8$	Asymptotic Holtsmark
10	5.371	5.126	4.878	4.634	5.563
12	3.303	3.182	3.053	2.926	3.392
14	2.196	2.148	2.077	1.996	2.249
16	1.567	1.526	1.475	1.428	1.583
18	1.151	1.127	1.100	1.068	1.164
20	0.876	0.858	0.841	0.822	0.886
22		0.680	0.664	0.643	0.692
24			0.528	0.519	0.554
26			0.441	0.432	0.451
28				0.354	0.373
30					0.313
35					0.212
40					0.151
45					0.112
50					0.086

for $P(\epsilon)$, valid for large values of ϵ , we follow Broyles⁴ and Mayer⁵ and assume that in this high-field region, only the nearest neighbor to an ion makes an appreciable contribution to the electric field at that ion. Thus we can relate $P(\epsilon)$ to the probability density $P(r) = 4\pi r^2 n g(r)$ that an ion will be at a distance r from any other ion; as a matter of convenience the ion at which the field distribution is being calculated is located at the origin of the r reference frame. Here, n is the ion density in the plasma and $g(r)$ is the well-known radial distribution function. Rigorously, we should use the probability of the nearest neighbor lying at a distance r from the ion instead of $g(r)$; however, when one of the ions is close to another, resulting in a large field, the difference between these two probabilities should be small. Since we are dealing with the low-frequency component, the ions interact with one another through a Debye-Hückel shielded potential and hence the electric field due to such a shielded ion is given by

$$\epsilon = (1/r^2)[1 + ar]e^{-ar}, \quad (2)$$

$$a \equiv r_0/\lambda,$$

where r_0 is the ion-sphere radius defined by

$$\frac{4}{3}\pi r_0^3 n = 1;$$

λ is the Debye length defined by

$$\lambda = (kT/4\pi n e^2)^{1/2},$$

and ϵ is measured in units of ϵ_0 , the normal field strength,

$$\epsilon_0 = e/r_0^2.$$

Then

$$d\epsilon = (a/r)e^{-ar}[2 + (2/ar) + ar]dr. \quad (3)$$

⁴ A. A. Broyles, Phys. Rev. **100**, 1181 (1955).

³ B. Mozer, dissertation, Carnegie Institute of Technology, 1960 (unpublished).

⁵ H. Mayer, Los Alamos Scientific Laboratory Report No. LA-647, 1947 (unpublished).

TABLE II. Probability distributions $10^3 P(\epsilon)$ at a charged point, for several values of a . The electric-field strength ϵ is expressed in units of ϵ_0 . In each of the $10^3 P(\epsilon)$ columns, all values of $10^3 P(\epsilon)$ in italics have been calculated using the asymptotic expression, Eq. (6), of the text. The shift from the nearly exact results to the asymptotic involves, at most, an error of a few percent.

ϵ	$a=0.2$	$a=0.4$	$a=0.6$	$a=0.8$
10	5.177	4.481	3.674	2.881
12	3.171	2.730	2.208	1.689
14	2.115	1.816	1.453	1.106
16	1.484	1.265	1.000	0.738
18	1.094	0.928	0.725	0.522
20	0.829	0.689	0.540	0.384
22	0.650	0.546	0.405	0.290
24	0.517	0.427	0.318	0.224
26	0.426	0.339	0.255	0.176
28	0.344	0.279	0.207	0.141
30	0.283	0.232	0.171	0.114
35	0.192	0.154	0.110	0.071
40	0.137	0.108	0.075	0.047
45	0.101	0.079	0.054	0.032
50	0.077	0.060	0.040	0.023

Again noting that ϵ is measured in units of ϵ_0 and r in units of r_0 , we may write

$$P(\epsilon)d\epsilon = 3r^2 g(r) dr. \quad (4)$$

For $g(r)$, we use³

$$g(r) = \exp[-(a^2/3r)e^{-\sqrt{2}ar}], \quad (5)$$

which is the appropriate Debye-Hückel expression. Hence, combining Eqs. (3)-(5), we arrive at the expression

$$P(\epsilon) = \frac{3r^2 \exp[-(a^2/3r)e^{-\sqrt{2}ar}]}{[2 + (2/ar) + ar](a/r^2)e^{-ar}}. \quad (6)$$

Note that unlike the Holtsmark expression, used for the neutral-point case, the charged-point asymptotic expression is dependent on the appropriate a value. Comparison of the charged-point values, calculated from the formalism developed in II, with the asymptotic expression calculated with Eq. (6), indicates that for all values of a treated here, $P(\epsilon)$ coincides with the asymptotic expression by the time $\epsilon=30$, with at most a few percent uncertainty. An example of this coincidence is illustrated in Fig. 2. In all cases, the $P(\epsilon)$ values for ϵ in the 30-to-50 range can be found, using Eq. (6); in no case will these values differ by more than a few percent from those calculated with the more exact theory. In Table II, values of $P(\epsilon)$ for various charged-point cases are listed.

It is interesting to note that, contrary to the neutral-point case, the $P(\epsilon)$ values corresponding to the highest

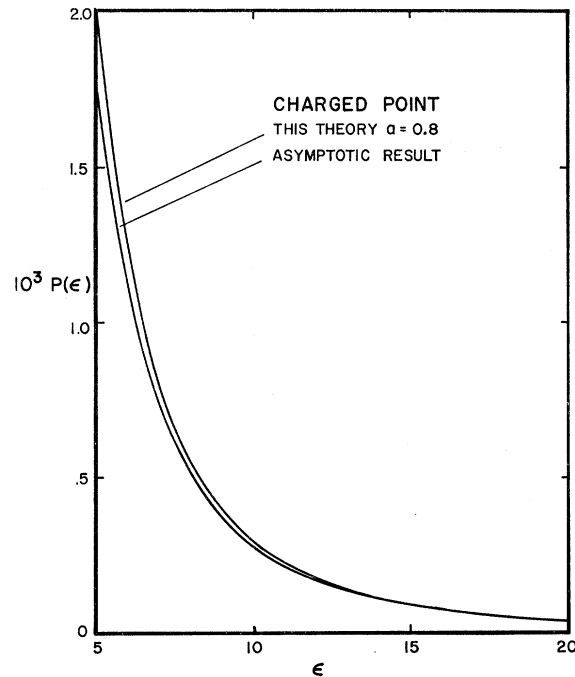


FIG. 2. A comparison of the charged-point electric microfield distribution calculated using the theory developed in II, with the asymptotic curve generated using Eq. (6); ϵ is in units of ϵ_0 .

a values most rapidly approach their asymptotic form. This verifies that the initial assumptions made in deriving the charged-point asymptotic form are applicable over the widest range of ϵ values in a high-density plasma.

Finally, as indicated in II, the asymptotic $P(\epsilon)$ curve can, with a high degree of accuracy, be calculated, using only the first approximation to the theory: that is, by using Eqs. (1), (16), (17) in II. Calculations show that the correction to $P(\epsilon)$ values, presented in this paper, brought about by inclusion of the second approximation to this theory does not exceed 3% for ϵ in the range from 10 to 30.

III. CONCLUSION

The results described in this paper will allow low-frequency-component $P(\epsilon)$ values to be calculated accurately for ϵ in the range 10 to 50. Both charged-point and neutral-point cases are treated. These results will enable more accurate calculations to be made of plasma-broadened spectral line shapes—especially in their wings.